Comment

Supplementary information to:

How climate change and unplanned urban sprawl bring more landslides

A Comment published in *Nature* **608**, 262–265 (2022)
https://doi.org/10.1038/d41586-022-02141-9

Ugur Ozturk, Elisa Bozzolan, Elizabeth A. Holcombe, Roopam Shukla, Francesca Pianosi & Thorsten Wagener

SUPPLEMENTARY INFORMATION

The following information in sections of Study Area, Data, and Methods, together with the Figures S1 to S6 and Table S1, constitutes the hypothesis of the main article. Here we cite more references on which the original study relies. This supporting document should be acknowledged along with the original article if the methods are of particular interest.

STUDY AREA

African urban centre Freetown from Sierra Leone is our flag case study. Freetown-Layered-Complex is the most common bedrock across Freetown Peninsula. The complex is a Mesozoic mafic intrusion as part of the early Jurassic African Craton [1,2]. The city is a major Atlantic port and had a population of about 1.2 million in 2020. The population has doubled since 1992 from 563,000, and it will feasibly double again by 2050, exceeding 2 million people [3]. The expanding city is progressively growing towards the landslide-prone hillslopes. Uncontrolled urban developments exacerbated the slope instability in recent years [4,5]. The city has recently experienced a major landslide disaster that killed about 1000 people [6,7].

The Caribbean Island Saint Lucia is our second case study. Deeply weathered and landslide-prone volcanic bedrocks and deep volcanic deposits compose the geology. Population in Saint Lucia is relatively steady; it was about 141,000 in 1992, and in 2020 around 180,000, and it will likely remain constant until 2050. Landslides in Saint Lucia are mostly rainfall-induced [8], just as in Freetown. Deforestation and informal urbanisation expansion have been recognised as the most significant contributors to risk from losses despite the meagre rise in the population [9].

DATA

Disaster risk reduction (DRR) experts need to consider 'dynamic' interactions between changing rainfall patterns, slope stability mechanisms, and urbanisation practices that modify triggers, land cover, slope angles, and drainage over time [10]. As a showcase, we adopted several globally available datasets to demonstrate that people living in informal settlements with poor building practices are more exposed to landslides. We further combined these data with mechanistic models to estimate the impact of informal building practice as a landslide cause, besides increasing extreme rainfall events due to climate change.

Population: The base population we refer to is the 1990 urban population provided by the UN-DESA [11]. However, the land cover products were delivered from 1992 onwards (further explained below). Hence, we link the 1990 population to the 1992 urban area in our analyses. Kii [3] projected the urban populations based on “Population of Urban Agglomerations with 300,000 Inhabitants or More in 2018” [11] following Shared Socioeconomic Pathways (SSPs). The projections by Kii [3] also rely on version 4 (v4) of the Gridded Population of the World [12,13]. We used the population estimates based on the fourth scenario (SSP4) that assumes unequal, stratified economies with rapid (moderate) urbanisation in medium- and low-income (high-income) countries. SSP4 realistically assumes the urban population to increase mainly in high-fertility countries, reflecting the past emergence of urban centres in sub-Saharan Africa with 1–5 million residents. Those urban centres either host considerable informal settlements already, or informal settlements are likely to develop in their perimeter. More optimistic SSP1 and SSP5 project homogenous urbanisation in countries with different economic growth, while SSP2 and SSP3 assume intermediate economic growth with slow urbanisation.

Population projections by Kii [3] bring along uncertainties arising from the variations in future social, political, and environmental conditions related to the underlying SSPs [14]. Hence, the study assessed the projection uncertainties by estimating the absolute percentage errors (APEs) of the projections by comparing them to the urban population provided by the UN-

DESA [11], which is available only until 2035. The reported error logically increases with time from 10% for 10-year to 16% for 25-year projections.

The example emphasizing the population living on steep terrain in Caracas and Taiz is based on the work of the Pesaresi et al. [15].

DEM: Digital elevation model (DEM) of the NASA Shuttle Radar Topographic Mission (SRTM) forms the basis for our topographic analyses. Version 4.1 (v4.1) of the SRTM data covers over 80% of the globe in 90-metre resolution at the equator (3-arc seconds) [16]. This data is accessible via the USGS FTP server. We interpolated all the spatial data in our analyses using the nearest-neighbour interpolation to the DEM resolution for consistency. DEM derivatives, such as hillslope angle, are computed in metric units referring to the Universal Transverse Mercator (UTM) coordinates in their respective UTM zone using TopoToolbox [17]. We used this 90-metre resolution data in our global analyses. We referred to the 30-metre (1-arc second) version (SRTM-v3.0) of the same data in our mechanistic model—CHASM+ (Extended Combined Hydrology and Stability Model).

Land cover: We relied on the European Space Agency (ESA) global land cover classification (The Multi-Resolution Land Characteristics, MRLC v2.0.7) to assess the changes in the urban area. Annual MRLC maps come in 300-metre spatial resolution from 1992 onwards. Each pixel value corresponds to the label of a land cover class defined based on the UN Land Cover Classification System (LCCS) [18]. If the urban class items such as buildings are sparsely distributed in a pixel, MRLC tends not to classify them as urban [19]. Hence, the final MRLC products underestimate urbanised peri-urban space. Even if all the cities we have used as examples host large and dense informal neighbourhoods, we might still miss sparsely urbanised areas. This potential bias would likely lessen the representation of informal communities on steeper hillslopes, undermining the severity of the highlighted problem—urban population at risk—in this study.

Informal settlements: Informal settlements are those neighbourhoods with limited physical and socioeconomic access to the opportunities of their respective cities [20]. Using this feature of physical inaccessibility, Soman et al. [21] classified the neighbourhoods based on the number of building parcels, namely k-complexity, from the least accessible building in a street block to the nearest external street. Hence, informal neighbourhoods are classified not as binary units but measured on a gradient. The higher the number of building parcels, the more inaccessible the neighbourhood is. The OpenStreetMap (OSM) data is the basis of the building footprints and road networks [22]. The OSM mission covered more than 95% of all roads in about 42% of countries with an ~83% completeness globally [23]. Although OSM coverage varies between developed and developing countries, with heterogeneous urban and rural areas [e.g., 24], high-density urban areas are covered considerably better [25]. Considering the variety in the completeness of OSM data [21], we used only those cities with high coverage as case studies [e.g., 22]. For Freetown (Sierra Leone), we used an upgraded version of the original data provided by Mansueto Institute analysis of OpenStreetMap [26].

Landslides data: Our motivation regarding the fatal landslides hinge on Froude and Petley's [27] data. The original data covers the period from 2004 to 2018, with recent updates in AGU Landslide Blog by Dave Petley [e.g., 28]. The Global Fatal Landslide Database (GFLD) relies on English daily and systematic metadata search tools, such as news reports in mass media. We excluded landslides with natural triggers, such as earthquakes and rainfall, showing only the anthropogenic landslides (Figure S1).

The example about the landslide counts in (de)forested informal settlements in Rio de Janeiro, Brazil in the manuscript rely on the work of Smyth and Royle [29].

Input factors for CHASM+: CHASM+ (Extended Combined Hydrology and Stability Model) [30,31] requires information on two-dimensional slope cross-section geometry (e.g., hillslope angle, elevation, and depth of the strata), soil properties (geotechnical and hydrological),

boundary conditions (e.g., initial water table) and urban properties (cut slope angle, presence/absence of roof gutters, leaking pipes and septic tanks).

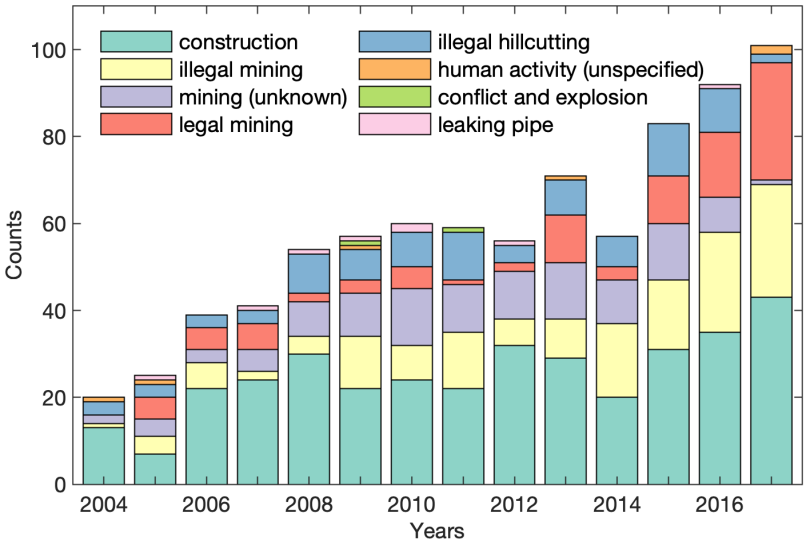

Figure S1. *Global fatal landslides without natural triggers between 2004 and 2017, such as earthquakes and rainfall [27]. Especially those landslides induced by mining, hillcutting, and construction are on the rise.*

For Freetown (the case study reported in the main manuscript), we obtained the input data and the associated probability distributions via literature and expert elicitation via collaboration with the engineering consultancy Arup [32–36]**.** For Saint Lucia (the case study reported in this supplementary information), primary inputs related to soil strength properties are shear tests of local soils [37,38] and similar volcanic tropical residual soils [39]. Soil and urban properties information were collated through community-based mapping and local experts [8]. The parameters of the probability distributions of these properties were extrapolated from this data as well as from the literature and they are reported in Bozzolan et al. [31]. However, here, we modified the variability range of the hillslope angle (between 10° and 35°) and included the vegetated hillslopes simulation. For both case studies analysed, the simulated synthetic natural hillslopes refer to fully vegetated hillslopes with shallow and deep roots (shrub and forest). CHASM+ represents vegetation via rainfall interception, evapotranspiration, root water uptake, vegetation surcharge, and increased permeability and soil cohesion due to the root network. We considered the vegetation properties invariant in the stochastic sampling [e.g., 40]—i.e., not accounting for their spatial variability and modifications due to climate change.

We represent informal housing by uncontrolled hill cutting, house loads, and lack of surface urban water management. These urban construction activities are described in CHASM+ by appropriately modifying the hillslopes' geometrical profile and by introducing roof gutters on houses, leaking superficial pipes, and buried septic tanks. Bozzolan et al. [31] report their variability ranges. Simulations also include variations in the housing density (from 1 to 100% of the hills urbanised).

Hourly rainfall intensity and duration are the dynamic forcing parameters in the CHASM+ model. We refer to intensity-duration-frequency (IDF) relationships derived from the design of the Roseau Dam in Saint Lucia [41]. We derived a minimum and maximum rainfall intensity and duration (with the maximum respectively 200 mm/h and 72h). Almeida et al. [42] suggested sampling from these ranges independently and uniformly (no a-priori-knowledge). Hence, we randomly generated a wide range of rainfall intensity-duration combinations to capture observed and likely future rainstorms. Given that no rainfall records were available for Freetown, we used the same variability ranges from Saint Lucia.

METHODS

Method 1 – Urban population & area: We calculated the annual urban population growth rate based on SSP4 data for every two latitudes (e.g., 0–2, 2–4) along the entire longitudinal

[-180 180] range to show the population growth rate on the latitudinal scale in Figure 1A (Original figure is shown here as Figure S2). Each city in a two-latitudinal interval has a different annual growth rate. Hence, we calculated the mean for each interval (points in Figure 1A) and included the Gaussian smoothed continuous mean as a line. The shaded area around the line continuously shows the growth rate variation. Using the MRLC data, we computed the spatial urban expansion rate for the same region (2 latitudes along the entire longitudinal range) in Figure 1B. We divided the classified metropolitan area in 2020 with the same in 1992 to highlight that the urban area has grown 2.38 times since 1992. We estimated the required new urban space to host the increasing population between 2020 and 2050, assuming simplistically concentric growth of the urban areas spatially controlled only by the topography. Method 3 further explains the computation details of the approach. The urban area in 2050 will be 3.18 times the area in 1992. Assuming a homogenous population distribution in the urban space, we could also anticipate the population in different hillslope ranges (Table 1).

Table S1. The population of tropical cities (>300K) in millions. We assume a homogeneously distributed population in classified urban areas.

Hillslope range	*0°--10°*	*10°--20°*	*20°--30°*	*30°--90°*
Population in 1990	*401,9*	*7,3*	*1*	*0,2*
Population in 2020	*2755,7*	*55,1*	*7,6*	*1,8*
Population in 2050	*3727,8*	*80*	*11,1*	*2,5*

Alternative urban expansion projections exist based on the SLEUTH urban growth model [43,44]. Underlying population estimates for these projections are approximately 1 km spatial resolution LandScan global population data by Oak Ridge National Laboratory https://landscan.ornl.gov/landscan-datasets). LandScan underestimates the population living in informal settlements [45–47]. In Addition, the earliest dated grid data is from 2010, which is relatively young compared to those based on MRLC. Considering the above-listed gaps, we have not referred to these projections of the SLEUTH model. Nevertheless, we show the urban hillslope distributions for 2050 normalised by the distribution of 2020 based on the SLEUTH model (Figure S2), which could be compared to Figure 1C.

Method 2 – Urban hillslope distribution in Tropics: A landslide is a downslope gravitational mass movement of earth materials. Hence the hillslope angle is the primary cause of landslides and is commonly attributed as the most critical covariate in susceptibility and hazard models [48]. To mimic the landslide-prone urban space, we controlled the urban slope distribution in tropical cities with a minimum of 300,000 inhabitants in 2018. We computed the density of urban areas along hillslopes [0° 35°] (bandwidth = 2) in the entire tropics. Dividing the urban slope distribution in 2020 with the one in 1992 helped highlight the elevated population expansion on landslide-prone steeper hillslopes (10°–35°) [49,50], when compared to the milder urban slopes (<10°) in Figure 1C. Below we also show the transitional change of urban hillslope distributions from 1992 to 2020 based on MRLC data (Figure S3). Besides our flag example of Freetown, we offer two hilly inland towns, Bukavu (DR Congo) in Africa and Medellin (Colombia) in South America. We choose Medellin and Bukavu as examples, while both these inland cities host rapidly expanding informal settlements with high landslide risk [e.g., 51,52]. The urban expansion towards steeper hillslopes is faster in Freetown, while the transition is more gradual in Bukavu and Medellin (Figure S3). Starting in the mid-2000s, Internal displacement following Sierra Leone's Civil War enhanced the development of informal settlements around the rugged perimeter of Freetown [53,54], steepening the urban hillslope distribution (Figure S2B').

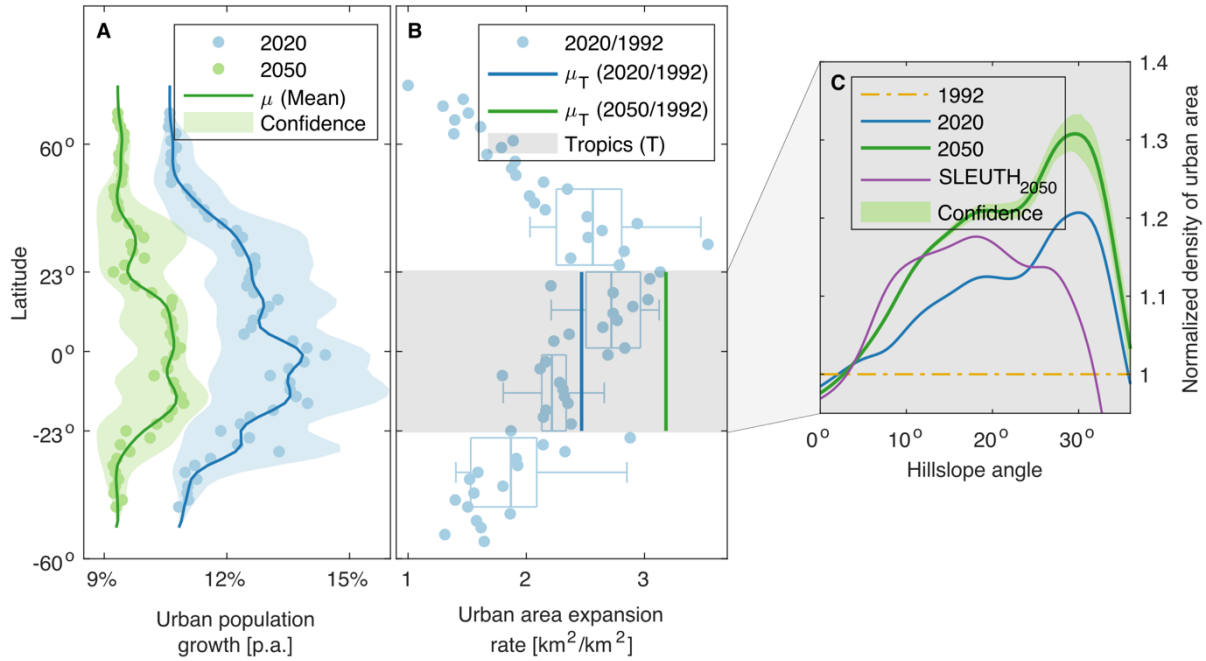

Figure S2: Extended version of the Figure 1 in the main manuscript. (A) includes also the projection of annual urban population growth rate in 2050. (B) Box plots highlight the variety of the scattered data of global urban growth as ratios of 2020 and 1992 in 4 equal latitudinal intervals between 46°N and 46°S. (C) The projected urban hillslope distributions of the SLEUTH model for 2050, which is normalized by the distribution of 2020 [43,44].

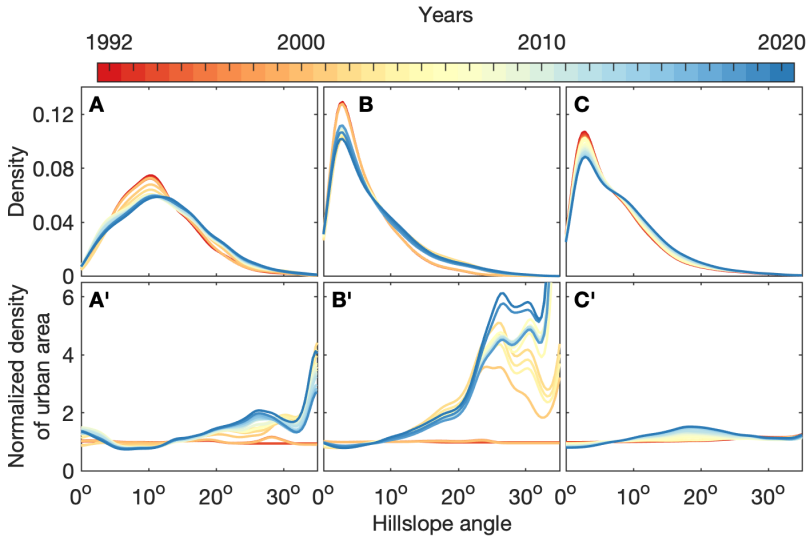

Figure S3. Urban hillslope angle distribution of (A, A') Bukavu (DR Congo) and (B, B') Freetown (Sierra Leone) in Africa, and (C, C') Medellin (Colombia) in South America over the last 29 years [1992–2020]. (A), (B), and (C) depict the actual hillslope distribution of the indexed year. (A'), (B'), and (C') show the hillslope distributions normalised by the distribution of 1992. The higher values of normalised density highlight those hillslope intervals where the urban expansion was more prominent.

Method 3 – Urban hillslope projection in Tropics: To project the slope distribution in 2050, we assumed homogeneous population density to simplify the computation. First, we estimated the required metropolitan area to accommodate the new population towards 2050 using the population (i.e., 1990) and urban area differences between 1992 and 2020, as mentioned previously in Method 1. This difference leads to assessing the required space in 2050, assuming no change in construction style (e.g., an increasing percentage of high-rise buildings). Then, we calculated the immediate nonurban area (grid cells, 300m×300m) encircling the urban area in 2020 to narrow the problem to which of the available grid cells will be occupied by the newly urbanised area. Instead of randomly selecting a sample from these available grid cells, we weighted them based on a suitability index (mean line in Figure S4) following the past land occupation behaviour. The tendency to settle on hillslopes decreases considerably should there be enough suitable gentle terrain (Figure S4). Based

on the mean behaviour over the last 28 years [1993–2020], we weighted our random sampling of the available terrain encircling the urban centres in 2020 to urbanise towards 2050. We sampled the required area to host the new population in 2050 from available grid cells 1000 times to estimate the uncertainty of our assumption (Figure 1C). As seen in the grey shaded area of the normalised density for 2050 in Figure 1C, the projection is consistent with respect to the 2020 situation. Densities in Figure 1C and wherever else used throughout the manuscript takes bandwidth as 2 to achieve comparable results.

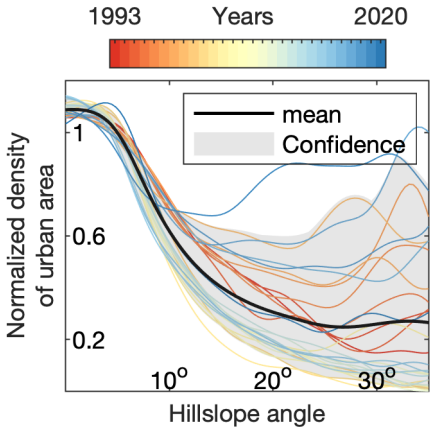

Figure S4. *Slope distribution of newly urbanised areas compared to the available adjacent space encircling the urban centres the year before over the last 28 years [1992–2020]. The shaded area highlights the 5th–95th percentile confidence.*

Method 4 – Hillslope distribution of informal neighbourhoods: We selected four emerging tropical towns distributed in 3 continents—Antipolo (Philippines) and Baguio (Philippines) in Asia, Port au Prince (Haiti) in the Caribbean, and Freetown (Sierra Leone) and Bukavu (DR Congo) in Africa—to show hillslope angles across different districts. Spanning through the entire tropical realm, rapidly evolving informal settlements of these case cities also have a high landslide risk [27,55]. We consistently distributed the integer values of k-complexity up to 9 in 4 subcategories while dividing the communities regardless of their spatial coverage of the total urban area. The k-complexity equal to or above 9 depicts the least accessible areas, the 5th subcategory. We categorised the k-complexity of 10–14 as the least accessible area to achieve a more homogenous subdivision of the total area in the case of Freetown (Figure 2A). The spatial coverage of each subcategory varies the least in Baguio (18%–24%) and the most in Antipolo (4%–43%). The distribution of hillslope angles shifts rightwards towards steeper hillslopes in more inaccessible (likely informal) parts of each city. Hence, more vulnerable people are exposed to landslides, potentially increasing the impact of future disasters [56]. They often also raise landslide hazard with unregulated deforestation, illegal slope cutting and terracing, and a lack of drainage [57].

Method 5 – Set up of the mechanistic model CHASM+: We quantified the role of informal housing in slope stability under different climate conditions by using the 2D mechanistic CHASM+ (Extended Combined Hydrology and Stability Model) [30,31]. CHASM+ temporally analyses slope stability under changes of slope hydrology. It relies on Bishop's circular limit equilibrium method [58], using rainfall intensity and duration as the dynamic slope destabilising force. In our case examples of Freetown (Sierra Leone) and Saint Lucia (Caribbean), the model inputs are the parameters defining the lithology, morphology, urban characteristics, and rainfall-forcing data (described in the previous section). We represent these parameters' variation and uncertainty across the two cities using their probability distributions. These distributions were assessed based on information available online, on literature and on the data collected from the field (also critically including previous studies within informal communities which provided information on soil strata depths, cut slope angles, and other types of urban construction practices). By sampling the model input in a Monte Carlo framework following their probability distributions, we obtained a library of about 120,000 simulations per case study, each one representing a feasible hillslope in the area (i.e., where for feasible we mean statistically possible, given that the hillslopes parameters are chosen as values of their probability distributions). We finally assessed the stability of these

hillslopes with CHASM+, obtaining a corresponding number of slope stability responses (i.e., the minimum factor of safety). Bozzolan et al. [31] provide more details on the model run in a stochastic framework.

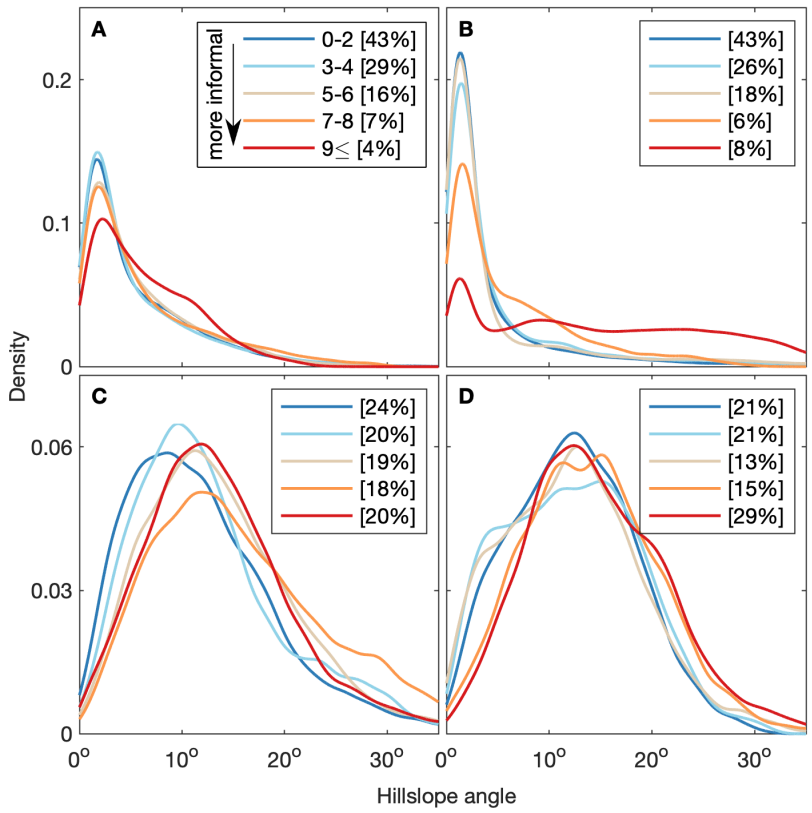

Figure S5. Hillslope angles across different districts. (A) Antipolo in the Philippines and (B) Port au Prince in Haiti have less informally urbanised areas with clearly different hillslope angle distributions. The distributions of (C) Baguio in the Philippines and (D) Bukavu in the DR Congo gradually shift rightwards with increasing informality. Slums are more likely to exist on hillslopes greater than 10°, increasing landslide exposure. The legend shows the number of building parcels a person has to cross to get to the nearest external street as a proxy of the quality of urbanisation: the higher the number, the more informal the neighbourhood. We provide the spatial coverage of each category in the urban area in brackets.

Once this library of slope stability response was available, we calculated the IDF curves associated with 100 years return period events based on the global data provided by Courty et al. [59]. We accounted for climate change impact by modifying these IDFs for the scenarios RCP8.5, as described by Martel et al. [60]. To generate Figure 2B in the main article (for Freetown) and Figure S6 below (for Saint Lucia), we selected the CHASM+ simulations associated with rainfall-durations combinations similar to these calculated IDFs.

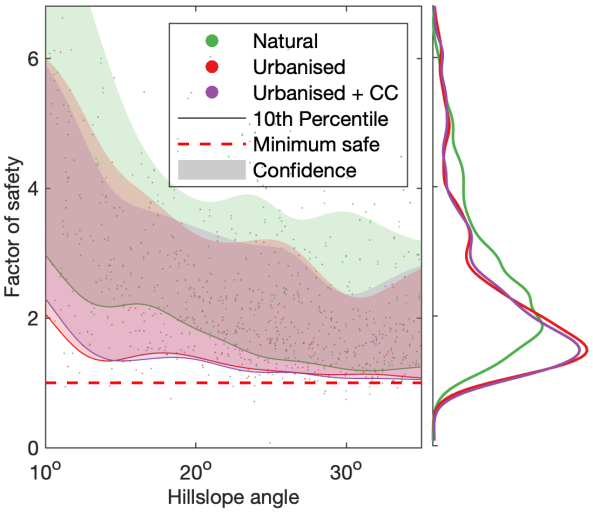

Figure S6. The likelihood of slope failure (FS < 1) along different hillslope angles considering the influence of informal housing and climate change (CC) for Saint Lucia in the Caribbean. The 10th–90th percentile range highlights the confidence band of our simulations. Marginal distributions along the vertical axes show the safety factors per category, which represents how the simulated slope stability responses (i.e., the dots in the background) distribute along the y-axis for the "Natural", "Urbanised", and "Urbanised with Climate Change" cases.

In both case studies, urbanisation is the main reason for decreasing slope stability [e.g., 29,61]. Although the Factor of safety (FS) remains largely above one even when we consider urbanisation, there is a significant decrease in the overall slope stability in Saint Lucia

(Figure S6). Another important aspect is that while the frequency of urban landslides increases, their dimensions (radius) decrease compared to natural hillslopes (see Figure S7 for Freetown and Figure 9 in Bozzolan et al. [31] for Saint Lucia). Therefore, the findings reflect the empirical evidence in low-income communities reporting a high frequency of small-scale landslides, particularly associated with cut slopes, for high intensity and short-duration events—"everyday extensive risks" [62,63].

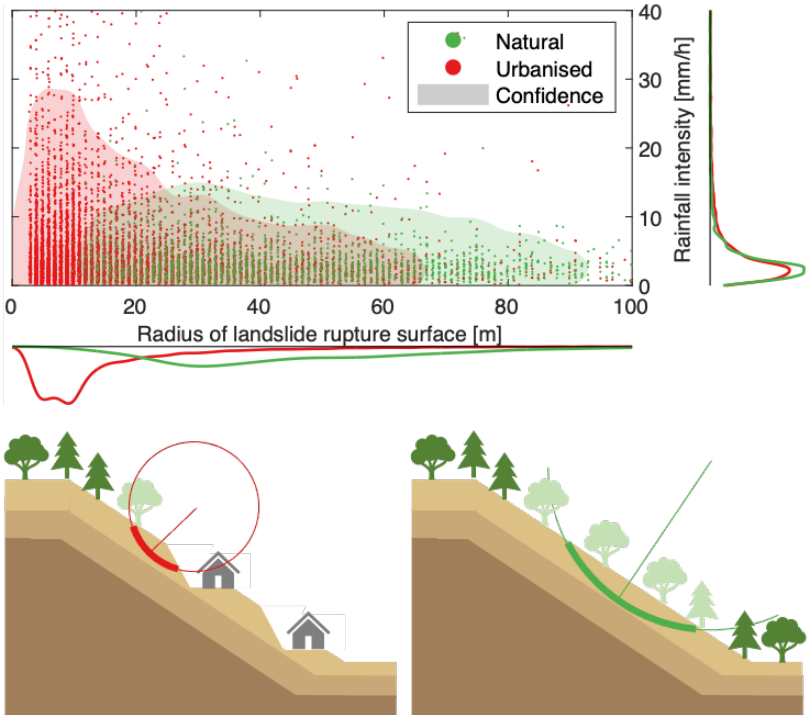

Figure S7. Landslide size distribution for natural and informally urbanised areas in Freetown. The shaded area covers 95% of simulated landslides in the respective category (i.e., urbanised or natural). Marginal distributions along both the axes show landslide rupture size and rainfall intensity, representing how the simulated slope stability response (i.e., dots in the background) distribute along the x- and y-axis for the 'Natural' and 'Urbanised' cases. The shaded area and the marginal distributions along the x-y axis highlight that the landslides get smaller and more frequent (+20%) in the informally urbanised landscape when compared to natural hillslopes.

These results account for the uncertainty in future urban development and climate change projections as well as in the inherent uncertainty in the hillslopes' soil properties and geotechnical characteristics. Identifying a trend in slope stability (e.g., a decrease in FS when informal urbanisation is present) over the variation and uncertainty of all these model's input factors, make the presented results robust. Nevertheless, here we show 'proof of concept' modelling results. Our simulations indicate likely trends and the value of the modelling approach; the outputs should not form the basis for policy in their current state.

ACKNOWLEDGEMENTS

UO is supported by the research focus point Earth and Environmental Systems of the University of Potsdam. UO and RS acknowledge support from the Co-PREPARE [57553291] of the German Academic Exchange Service (DAAD). FP is partially supported by the UK-EPSRC grant [EP/R007330/1]. TW acknowledges support from the Alexander von Humboldt Foundation in the framework of the Alexander von Humboldt Professorship endowed by the German Federal Ministry of Education and Research (BMBF). We thank ARUP for providing expert knowledge and data used in the mechanistic modelling of Freetown.

REFERENCES

1. Callegaro, S. *et al.* Geochemical Constraints Provided by the Freetown Layered Complex (Sierra Leone) on the Origin of High-Ti Tholeiitic CAMP Magmas. *Journal of Petrology* **58**, 1811–1840 (2017).
2. Chalokwu, C. I. Petrology of the freetown layered complex, Sierra Leone: part II. Magma evolution and crystallisation conditions. *Journal of African Earth Sciences* **32**, 519–540 (2001).

3. Kii, M. Projecting future populations of urban agglomerations around the world and through the 21st century. *npj Urban Sustain* **1**, 10 (2021).
4. Cui, W., Dong, X., Xi, B., Feng, Z. & Fan, J. Can the GPM IMERG Final Product Accurately Represent MCSs' Precipitation Characteristics over the Central and Eastern United States? *Journal of Hydrometeorology* **21**, 39–57 (2020).
5. Lahai, Y. A., Anderson, K. F. E., Jalloh, Y., Rogers, I. & Kamara, M. A comparative geological, tectonic and geomorphological assessment of the Charlotte, Regent and Madina landslides, Western area, Sierra Leone. *Geoenviron Disasters* **8**, 16 (2021).
6. Redshaw, P. *et al.* The 2017 Regent Landslide, Freetown Peninsula, Sierra Leone. *Quarterly Journal of Engineering Geology and Hydrogeology* **52**, 435–444 (2019).
7. Cui, Y. *et al.* The cost of rapid and haphazard urbanization: lessons learned from the Freetown landslide disaster. *Landslides* **16**, 1167–1176 (2019).
8. Anderson, M. G. & Holcombe, E. *Community-based landslide risk reduction: managing disasters in small steps*. (World Bank Publications, 2013).
9. World Bank. *Disaster Risk Management in Latin America and the Caribbean Region: GFDRR Country Notes*. https://openknowledge.worldbank.org/handle/10986/27336 (2012).
10. Depicker, A. *et al.* Historical dynamics of landslide risk from population and forest-cover changes in the Kivu Rift. *Nat Sustain* **4**, 965–974 (2021).
11. UN-DESA. *World Urbanization Prospects: The 2018 Revision. United Nations Department of Economic and Social Affairs*. (UN, 2019). doi:10.18356/b9e995fe-en.
12. Doxsey-Whitfield, E. *et al.* Taking Advantage of the Improved Availability of Census Data: A First Look at the Gridded Population of the World, Version 4. *Papers in Applied Geography* **1**, 226–234 (2015).
13. CIESIN. *Gridded population of the world, version 4 (GPWv4): Population density*. *NASA Socioeconomic Data and Applications Center (SEDAC)* (Center for International Earth Science Information Network-CIESIN-Columbia University, 2016).
14. Riahi, K. *et al.* The Shared Socioeconomic Pathways and their energy, land use, and greenhouse gas emissions implications: An overview. *Global Environmental Change* **42**, 153–168 (2017).
15. Pesaresi, M., Melchiorri, M., Siragusa, A. & Kemper, T. *Atlas of the human planet 2016: mapping human presence on Earth with the global human settlement layer.* https://data.europa.eu/doi/10.2788/889483 (2016).
16. Jarvis, A., Reuter, H. I., Nelson, A. & Guevara, E. Hole-filled SRTM for the globe Version 4, available from the CGIAR-CSI SRTM 90m Database. (2008).
17. Schwanghart, W. & Scherler, D. Short Communication: TopoToolbox 2 – MATLAB-based software for topographic analysis and modeling in Earth surface sciences. *Earth Surf. Dynam.* **2**, 1–7 (2014).
18. Defourny, P. ESA Land Cover Climate Change Initiative (Land_Cover_cci): Land Cover Maps. (2017).
19. Wickham, J., Stehman, S. V., Sorenson, D. G., Gass, L. & Dewitz, J. A. Thematic accuracy assessment of the NLCD 2016 land cover for the conterminous United States. *Remote Sensing of Environment* **257**, 112357 (2021).
20. Brelsford, C., Martin, T., Hand, J. & Bettencourt, L. M. A. Toward cities without slums: Topology and the spatial evolution of neighborhoods. *Sci. Adv.* **4**, eaar4644 (2018).
21. Soman, S., Beukes, A., Nederhood, C., Marchio, N. & Bettencourt, L. Worldwide Detection of Informal Settlements via Topological Analysis of Crowdsourced Digital Maps. *IJGI* **9**, 685 (2020).
22. OpenStreetMap. Planet dump retrieved from https://planet.osm.org. (2019).
23. Barrington-Leigh, C. & Millard-Ball, A. The world's user-generated road map is more than 80% complete. *PloS one* **12**, e0180698 (2017).
24. Zhang, Y., Li, X., Wang, A., Bao, T. & Tian, S. Density and diversity of OpenStreetMap road networks in China. *Journal of Urban Management* **4**, 135–146 (2015).

25. Meijer, J. R., Huijbregts, M. A., Schotten, K. C. & Schipper, A. M. Global patterns of current and future road infrastructure. *Environmental Research Letters* **13**, 064006 (2018).
26. Mansueto Institute analysis of OpenStreetMap. Database of Global Administrative Areas (GADM), and Ecopia. (2021).
27. Froude, M. J. & Petley, D. N. Global fatal landslide occurrence from 2004 to 2016. *Nat. Hazards Earth Syst. Sci.* **18**, 2161–2181 (2018).
28. Petley, D. Fatal landslides in 2019. *The Landslide Blog* https://blogs.agu.org/landslideblog/2020/03/25/2019-fatal-landslides/ (2022).
29. Smyth, C. G. & Royle, S. A. Urban landslide hazards: incidence and causative factors in Niterói, Rio de Janeiro State, Brazil. *Applied Geography* **20**, 95–118 (2000).
30. Anderson, M. G. & Lloyd, D. M. Using a Combined Slope Hydrology-Stability Model to Develop Cut Slope Design Charts. *Proceedings of the Institution of Civil Engineers* **91**, 705–718 (1991).
31. Bozzolan, E., Holcombe, E., Pianosi, F. & Wagener, T. Including informal housing in slope stability analysis–an application to a data-scarce location in the humid tropics. *NHESS* **20**, 3161–3177 (2020).
32. ALM *et al. The World Bank Sierra Leone Multi-City Hazard Review and Risk Assessment Final Report (Volume 4 of 5): Bo City Hazard and Risk Assessment*. https://www.worldbank.org/en/topic/disasterriskmanagement/brief/sierra-leone-multi-city-hazard-review-and-risk-assessment (2018).
33. Morley, A. *et al. The World Bank Sierra Leone Multi-City Hazard Review and Risk Assessment Final Report (Volume 2 of 5): Freetown City Hazard and Risk Assessment*. https://www.worldbank.org/en/topic/disasterriskmanagement/brief/sierra-leone-multi-city-hazard-review-and-risk-assessment (2018).
34. Campbell, G., Morley, A., Free, M., Bottomley, J. & Redshaw, P. *The World Bank Sierra Leone Multi-City Hazard Review and Risk Assessment Final Report (Volume 3 of 5): Makeni City Hazard and Risk Assessment*. https://www.worldbank.org/en/topic/disasterriskmanagement/brief/sierra-leone-multi-city-hazard-review-and-risk-assessment (2018).
35. Redshaw, P., Bottomley, J., Campbell, G., Morley, A. & Free, M. *The World Bank Sierra Leone Multi-City Hazard Review and Risk Assessment Final Report (Volume 1 of 5): Technical Methodology and Summary of Results*. https://www.worldbank.org/en/topic/disasterriskmanagement/brief/sierra-leone-multi-city-hazard-review-and-risk-assessment (2018).
36. Redshaw, P., Anna Morley & Free, M. *The World Bank Sierra Leone Multi-City Hazard Review and Risk Assessment Final Report (Volume 5 of 5): Map Volume*. https://www.worldbank.org/en/topic/disasterriskmanagement/brief/sierra-leone-multi-city-hazard-review-and-risk-assessment (2018).
37. Anderson, M. G. & Kemp, M. J. *The prediction of pore water pressure conditions in road cut slopes, St Lucia, West Indies*. (Overseas Development Agency, London, UK, Final Technical Report, 1985).
38. Holcombe, E. A. Modelling landslide risk on highway cut slopes in developing countries. (University of Bristol, 2006).
39. Anderson, M. G. & Howes, S. Development and application of a combined soil water-slope stability model. *Quarterly Journal of Engineering Geology and Hydrogeology* **18**, 225–236 (1985).
40. Holcombe, E. A., Beesley, M. E. W., Vardanega, P. J. & Sorbie, R. Urbanisation and landslides: hazard drivers and better practices. *Proceedings of the Institution of Civil Engineers - Civil Engineering* **169**, 137–144 (2016).
41. Klohn-Crippen. *Roseau Dam and ancillary works, Tropical storm Debbie*. (1995).
42. Almeida, S., Holcombe, E. A., Pianosi, F. & Wagener, T. Dealing with deep uncertainties in landslide modelling for disaster risk reduction under climate change. *Nat. Hazards Earth Syst. Sci.* **17**, 225–241 (2017).

43. Zhou, Y., Varquez, A. C. G. & Kanda, M. High-resolution global urban growth projection based on multiple applications of the SLEUTH urban growth model. 1021279858 Bytes (2019) doi:10.26188/5C2C5D0ED52D7.
44. Zhou, Y., Varquez, A. C. G. & Kanda, M. High-resolution global urban growth projection based on multiple applications of the SLEUTH urban growth model. *Sci Data* **6**, 34 (2019).
45. Dugoua, E., Kennedy, R. & Urpelainen, J. Satellite data for the social sciences: measuring rural electrification with night-time lights. *International journal of remote sensing* **39**, 2690–2701 (2018).
46. McMichael, C., Dasgupta, S., Ayeb-Karlsson, S. & Kelman, I. A review of estimating population exposure to sea-level rise and the relevance for migration. *Environ. Res. Lett.* **15**, 123005 (2020).
47. Thomson, D. R. *et al.* Evaluating the Accuracy of Gridded Population Estimates in Slums: A Case Study in Nigeria and Kenya. *Urban Science* **5**, 48 (2021).
48. Ozturk, U., Saito, H., Matsushi, Y., Crisologo, I. & Schwanghart, W. Can global rainfall estimates (satellite and reanalysis) aid landslide hindcasting? *Landslides* (2021) doi:10.1007/s10346-021-01689-3.
49. Marc, O. *et al.* Initial insights from a global database of rainfall-induced landslide inventories: the weak influence of slope and strong influence of total storm rainfall. *Earth Surf. Dynam.* **6**, 903–922 (2018).
50. Prancevic, J. P., Lamb, M. P., McArdell, B. W., Rickli, C. & Kirchner, J. W. Decreasing Landslide Erosion on Steeper Slopes in Soil-Mantled Landscapes. *Geophys. Res. Lett.* **47**, (2020).
51. Nobile, A. *et al.* Multi-Temporal DInSAR to Characterise Landslide Ground Deformations in a Tropical Urban Environment: Focus on Bukavu (DR Congo). *Remote Sensing* **10**, 626 (2018).
52. Smith, H., Coupé, F., Garcia-Ferrari, S., Rivera, H. & Castro Mera, W. E. Toward negotiated mitigation of landslide risks in informal settlements: reflections from a pilot experience in Medellin, Colombia. *E&S* **25**, art19 (2020).
53. Rigon, A., Walker, J. & Koroma, B. Beyond formal and informal: Understanding urban informalities from Freetown. *Cities* **105**, 102848 (2020).
54. Silvério Marques, J., Van Dyck, J., Namara, S., Costa, R. & Bailor, S. *Sierra Leone Social Protection Assessment*. http://hdl.handle.net/10986/18966 (2013).
55. Patel, R. B. & Gleason, K. M. The association between social cohesion and community resilience in two urban slums of Port au Prince, Haiti. *International Journal of Disaster Risk Reduction* **27**, 161–167 (2018).
56. Raju, E., Boyd, E. & Otto, F. Stop blaming the climate for disasters. *Communications Earth & Environment* **3**, 1 (2022).
57. UN-Habitat. *The challenge of slums: global report on human settlements by United Nations Human Settlements Programme*. (Earthscan Publications, 2003).
58. Bishop, A. W. The use of the Slip Circle in the Stability Analysis of Slopes. *Géotechnique* **5**, 7–17 (1955).
59. Courty, L. G., Wilby, R. L., Hillier, J. K. & Slater, L. J. Intensity-duration-frequency curves at the global scale. *Environ. Res. Lett.* **14**, 084045 (2019).
60. Martel, J.-L., Brissette, F. P., Lucas-Picher, P., Troin, M. & Arsenault, R. Climate Change and Rainfall Intensity–Duration–Frequency Curves: Overview of Science and Guidelines for Adaptation. *J. Hydrol. Eng.* **26**, 03121001 (2021).
61. Petley, D. N. *et al.* Trends in landslide occurrence in Nepal. *Nat Hazards* **43**, 23–44 (2007).
62. Bull-Kamanga, L. *et al.* From everyday hazards to disasters: the accumulation of risk in urban areas. *Environment and Urbanization* **15**, 193–204 (2003).
63. Hamdan, F. Intensive and extensive disaster risk drivers and interactions with recent trends in the global political economy, with special emphasis on rentier states. *International Journal of Disaster Risk Reduction* **14**, 273–289 (2015).